ELSEVIER

Advances in Water Resources 24 (2001) 1143–1157

Advances in Water Resources

www.elsevier.com/locate/advwatres

Soil moisture variability and scale-dependency of nonlinear parameterizations in coupled land–atmosphere models

Deborah K. Nykanen *,[1], Efi Foufoula-Georgiou

St. Anthony Falls Laboratory, Department of Civil Engineering, University of Minnesota, Mississippi River at Third Avenue SE, Minneapolis, MN 55414, USA

Received 23 August 2000; received in revised form 22 February 2001; accepted 14 March 2001

Abstract

Many of the relationships used in coupled land–atmosphere models to describe interactions between the land surface and the atmosphere have been empirically parameterized and thus are inherently dependent on the observational scale for which they were derived and tested. However, they are often applied at scales quite different than the ones they were intended for due to practical necessity. In this paper, a study is presented on the scale-dependency of parameterizations which are nonlinear functions of variables exhibiting considerable spatial variability across a wide range of scales. For illustration purposes, we focus on parameterizations which are explicit nonlinear functions of soil moisture. We use data from the 1997 Southern Great Plains Hydrology Experiment (SGP97) to quantify the spatial variability of soil moisture as a function of scale. By assuming that a parameterization keeps its general form the same over a range of scales, we quantify how the values of its parameters should change with scale in order to preserve the spatially averaged predicted fluxes at any scale of interest. The findings of this study illustrate that if modifications are not made to nonlinear parameterizations to account for the mismatch of scales between optimization and application, then significant systematic biases may result in model-predicted water and energy fluxes.

1. Introduction

The importance of incorporating land–atmosphere interactions in mesoscale and climate-scale atmospheric model predictions has gained increasing recognition over the past decade. In response, hydrological parameterizations developed for small (catchment) scales have been coupled to atmospheric models which are applied at grid scales ranging from several kilometers to hundreds of kilometers. The converse problem is that as computing resources have allowed the resolution of climate-scale models to be significantly increased, bucket-type hydrologic parameterizations developed for global scales are being applied to much smaller scales than those for which they were intended. In many cases, no modifications are made to the land-surface schemes to account for the change in scale of application. In other cases, ad hoc or empirical modifications (e.g., calibration) are made to parameterizations in an attempt to balance the water and energy budgets at a desired scale.

There are fundamental problems with applying catchment scale hydrological parameterizations to mesoscale or climate scales, and vice versa. Many of the variables involved have pronounced spatial variability which changes with scale, i.e., the resolution of the hydrologic or coupled model. Furthermore, many of the relationships describing land-surface hydrological processes and land–atmosphere interactions are nonlinear and thus statistical moments of large-scale averages (pixel values) depend on the small-scale (within pixel) variability of the variables involved. The combination of nonlinearity and spatial variability makes the parameterizations strongly dependent on the scale at which the process is considered, i.e., the model grid-size (see also discussion in [6]).

The purpose of this study is to investigate the sensitivity of nonlinear parameterizations used in coupled land–atmosphere models to the spatial variability of the involved variables and the degree of nonlinearity of the parameterizing equation. We focus on

* Corresponding author. Tel.: +1-906-487-3140; fax: +1-906-487-2943.

E-mail addresses: dnykanen@mtu.edu (D.K. Nykanen), efi@t-c.umn.edu (E. Foufoula-Georgiou).

[1] Now at: Department of Civil and Environmental Engineering, Michigan Technological University, Houghton, MI, USA.

0309-1708/01/$ - see front matter
PII: S0309-1708(01)00046-X

parameterizations which are explicit functions of soil moisture, a key variable in land–atmosphere interactions. Soil moisture is used in land-surface parameterization schemes to determine the sustainable evapotranspiration, ground temperature, partitioning of precipitation into infiltration and runoff, and partitioning of incoming solar energy between sensible and latent heat fluxes. Many of the hydrologic predictive equations involving soil moisture are nonlinearly parameterized and are consequently sensitive to the spatial variability of soil moisture and how this variability changes with scale.

Numerous studies have explored the natural variability of soil moisture and its scale-dependency. Rodriguez-Iturbe et al. [17] found that the variance of soil moisture in the surface layer follows a power law decay with increasing scale between 30 m and 1 km. Hu et al. [11] found a similar scaling relationship and extended it up to scales of 4.4 km. Cosh and Brutsaert [4] used semivariogram analysis to study the statistical and fractal characteristics of soil moisture. Famiglietti et al. [8] used both airborne remotely sensed measurements and impedance probe data to investigate the within-pixel variability of remotely sensed soil moisture. Other studies have investigated the effect of soil moisture variability on surface runoff generation, evapotranspiration, partitioning of incoming solar radiation between sensible and latent heat fluxes and found that including versus omitting this variability played an important role in model predictions (e.g., [1,7,14]; among others). Chen and Avissar [2,3] established a link between variability in soil moisture and the atmospheric response. They studied the impact of large-scale (80–240 km) discontinuities in soil moisture and found that it can generate mesoscale circulations and enhance cloud formation and associated precipitation.

The effect of spatial variability in other key land–atmosphere variables on model predictions has also been investigated by numerous studies. Ghan et al. [10] performed a systematic evaluation of the sensitivity of land-surface schemes to spatial variability in precipitation, vegetation, soil properties, solar radiation, and wind. They quantified the effect of including or omitting small-scale heterogeneity by comparing the predicted surface runoff and evaporation at larger scales. Sivapalan and Woods [18] studied the effect of spatial variability in precipitation on surface runoff, soil moisture, and evapotranspiration. Su et al. [19] explored the effect of aggregating radiative versus aerodynamic fluxes on the predicted areal average net radiation, ground heat flux, and sensible and latent heat fluxes. Nykanen et al. [16] studied the nonlinear propagation of small-scale rainfall variability through the coupled land–atmosphere system and found that including versus omitting small-scale variability in rainfall, and consequently in soil moisture, impacted the spatial organization of larger-scale land–atmosphere fluxes.

Since there is enough evidence to suggest that keeping parameterizations constant over a wide range of scales introduces considerable biases in the predicted fluxes, one could argue that an inverse approach of studying how parameterizations should change with scale such that fluxes of interest are preserved would be of practical interest. For some of these parameterizations, it could be possible to derive relationships between the grid scale of the model and the parameter value needed to preserve the average fluxes at a scale of interest. This is the conceptual approach followed in this study and emphasis is given on parameterizations that explicitly depend on soil moisture.

This paper is structured as follows. In Section 2, the theoretical framework for studying the scale-dependency of nonlinear parameterizations is presented in detail. In Section 3, the spatial variability of soil moisture is studied and characterized over scales of approximately 1–50 km using remotely sensed soil moisture data from the 1997 Southern Great Plains Hydrology Experiment (SGP97). The scale-dependency of nonlinear parameterizations is quantified in Section 4 by combining the developed theoretical framework and the observed scale-dependency of soil moisture variability. A summary of the results and conclusions are provided in Section 5.

2. Theoretical basis for the scale-dependency of nonlinear parameterizations

2.1. Development of equations

The main goal of this study is to investigate the scale-dependency of nonlinear parameterizations which depend on a variable that has considerable spatial variability over a range of scales. We focus on parameterizations which are explicit functions of soil moisture since, as discussed in Section 1, soil moisture has considerable spatial variability and is a key variable in hydrologic predictive equations. Since many soil moisture parameterizations can (at least over a range of scales) be approximated sufficiently well by combinations of power laws, we adopt here a nonlinear relationship of the form:

$$F \sim s^{\alpha}, \tag{1}$$

where F is a predicted flux, s is soil moisture and α is a parameter. Here, we denote by s the relative soil moisture within the upper 5 cm surface layer. Depending on the particular parameterization, however, s could be representative of a deeper layer of soil or refer to the volumetric soil moisture. This type of relationship is common in hydrologic prediction. It is used, for example, in the Biosphere–Atmosphere Transfer Scheme (BATS) land-surface model [5] in computing surface

runoff production, sustainable evapotranspiration, internal soil water fluxes, and thermal conductivity of the soil.

Let us assume that the parameter α is not a constant, but depends on the scale at which the predicted variable F is considered. Let λ_o denote the scale at which the parameterization was optimized, that is, the scale at which predicted fluxes from Eq. (1) were close in some statistical sense to the observed fluxes. Then recognizing the dependency on the scale λ_o, the power law relationship of (1) can be written as

$$F_{\lambda_o} \sim s_{\lambda_o}^{\alpha_{\lambda_o}}, \tag{2}$$

where α_{λ_o} denotes the parameter value at scale λ_o, s_{λ_o} the soil moisture at scale λ_o, and F_{λ_o} the value of a flux (e.g., runoff, evapotranspiration, heat flux) at scale λ_o as predicted by a model run at resolution λ_o. The parameterization is nonlinear when α_{λ_o} is not equal to 1.

There are several approaches that could be used to study the scale-dependency of nonlinear parameterizations like the one given in Eq. (2). One approach would be to apply the parameterization at scale λ_o and also at some other scale $\lambda \neq \lambda_o$ keeping the value of the parameter α_{λ_o} the same. The differences in the areal average model-predicted fluxes between the two simulations would provide insight on the sensitivity of the model to scale and the spatial variability of soil moisture. As discussed in Section 1, numerous studies have taken this approach to study the role of spatial variability of soil moisture and other variables in hydrologic and atmospheric predictions. Alternatively, one could proceed by assuming that the parameterization keeps the same form at all scales but not the same value of its parameters and study how the parameters should change with scale in order to preserve the areal average fluxes at the scale of interest. This is the approach followed here and is along the same lines as calibrating a model at different scales and seeing how the calibrated parameters change with scale.

Let λ denote some scale not equal to λ_o, α_λ the value of the parameter at scale λ, s_λ the soil moisture at scale λ, and F_λ the value of a flux predicted by the model run at resolution λ. The value of the parameter α_λ needed to preserve the areal average flux will be quantified for different scales λ as a function of α_{λ_o} and the scale-dependent spatial variability of the soil moisture field. We differentiate between two distinct cases:

(a) the case of applying the model at scales larger than the one for which its parameterizations were optimized (i.e., $\lambda > \lambda_o$) which is shown schematically in Fig. 1(a);

(b) the case of applying the model at scales smaller than the one for which its parameterizations were optimized (i.e., $\lambda < \lambda_o$) which is shown schematically in Fig. 1(b).

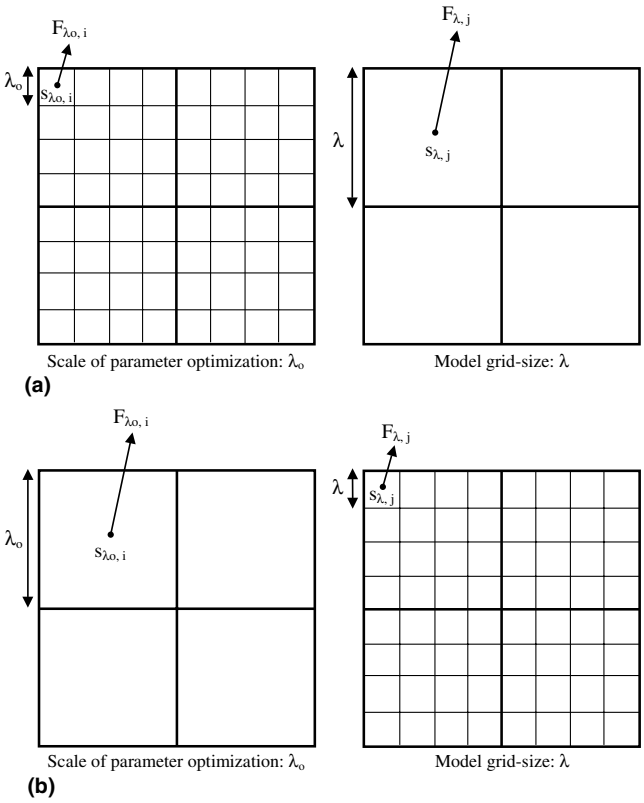

Fig. 1. Schematic of the case (a) $\lambda > \lambda_o$ and (b) $\lambda < \lambda_o$, where λ is the scale of the model and λ_o is the scale of parameter optimization. When the model is applied at scale λ which is larger than the scale of parameter optimization λ_o (upper panel), the original parameter of the model α_{λ_o} must change such that either (1) the fluxes $F_{\lambda,j}$ at every box of size λ are preserved (in which case a spatially variable parameter $\alpha_{\lambda,j}$ must be applied) or (2) the fluxes at scale λ are preserved on the average over a desired space–time domain (in which case a single effective parameter $\alpha_{\lambda,\mathrm{eff}}$ results). Similar constraints are also used in the case shown in the lower panel.

(a) *Case of* $\lambda > \lambda_o$

For the case of applying the model at scales larger than the one for which its parameterizations were optimized, the constraint is to preserve the spatial average flux within each grid box of size λ. Here, λ is the model grid-size and the scale of parameter optimization λ_o corresponds to a "subgrid-scale". Denoting by n the number of λ_o size pixels contained within a grid box of size λ and $\langle F_{\lambda_o}\rangle_{\lambda,j}$ the spatial average of the λ_o scale fluxes over grid box j of size λ, preservation of fluxes requires

$$F_{\lambda,j} = \frac{1}{n}\sum_{i=1}^{n} F_{\lambda_o,i} = \langle F_{\lambda_o}\rangle_{\lambda,\,j}. \tag{3}$$

Substituting in the above equation the fluxes in terms of the soil moisture at the appropriate scale and assuming that the proportionality factor of (1) is a constant (Appendix A examines a more general case in which the proportionality factor is a scale-dependent spatial field), we obtain

$$s_{\lambda,j}^{\alpha_{\lambda,j}} = \langle s_{\lambda_o}^{\alpha_{\lambda_o}} \rangle_{\lambda,j}. \quad (4)$$

Note that the spatial average of soil moisture at scale λ_o over model grid-size λ is the same as the value of soil moisture seen at scale λ, that is,

$$s_{\lambda,j} = \langle s_{\lambda_o} \rangle_{\lambda,j}. \quad (5)$$

The constraint equation (4) can be applied at each grid box j of size λ to find the parameter $\alpha_{\lambda,j}$ which preserves the flux $\langle F_{\lambda_o} \rangle_{\lambda,j}$ at that grid box. This would give a spatial distribution of α_λ across the domain as will be presented later.

Alternatively, one could find an "effective" parameter α (denoted as $\alpha_{\lambda,\mathrm{eff}}$), which preserves the flux $\langle F_{\lambda_o} \rangle_{\lambda,j}$ on the average over all j grid boxes of a desired space–time domain by taking the expectation over space and time,

$$E[s_\lambda^{\alpha_{\lambda,\mathrm{eff}}}] = E[s_{\lambda_o}^{\alpha_{\lambda_o}}]. \quad (6)$$

Using Taylor series expansion of the function $f(s) = s^\alpha$ around the mean $E[s]$ and taking expected values, we arrive at the known equation

$$E[f(s)] = f(E[s]) + \frac{f''(E[s])}{2}\mathrm{VAR}[s] + \frac{f'''(E[s])}{6} \times E[(s - E[s])^3] + \cdots \quad (7)$$

Ignoring higher order terms and evaluating the second derivative of $f(s)$ at $E[s]$ we obtain

$$E[s^\alpha] \cong E[s]^\alpha + \tfrac{1}{2}\mathrm{VAR}[s](\alpha - 1)\alpha E[s]^{(\alpha-2)}. \quad (8)$$

It is noted that keeping higher order terms in (7) does not present any technical difficulty but makes the relationships more cumbersome to follow. Applying (8) to (6) gives

$$E[s_\lambda]^{\alpha_{\lambda,\mathrm{eff}}} \cong E[s_{\lambda_o}]^{\alpha_{\lambda_o}} + \tfrac{1}{2}\mathrm{VAR}[s_{\lambda_o}](\alpha_{\lambda_o} - 1)\alpha_{\lambda_o} E[s_{\lambda_o}]^{(\alpha_{\lambda_o}-2)} - \tfrac{1}{2}\mathrm{VAR}[s_\lambda](\alpha_{\lambda,\mathrm{eff}} - 1)\alpha_{\lambda,\mathrm{eff}} E[s_\lambda]^{(\alpha_{\lambda,\mathrm{eff}}-2)}. \quad (9)$$

For a specified space–time domain and scales λ_o and λ, the variance and expectation of soil moisture can be computed and Eq. (9) can be solved iteratively for $\alpha_{\lambda,\mathrm{eff}}$. Notice that when the scale-dependency of a nonlinear parameterization is not considered, it is the terms involving $\mathrm{VAR}[s]$ in the above equation that are ignored. It is instructive to observe from Eq. (9) that in the limiting case when the grid-size of the model is equal to the scale at which the parameters were optimized ($\lambda = \lambda_o$), then the solution for $\alpha_{\lambda,\mathrm{eff}}$ would be α_{λ_o}, as expected. Otherwise if $\lambda \neq \lambda_o$, α_λ would differ from α_{λ_o} depending on how much the variability of the soil moisture field changes with scale. Notice also that if the parameterization was linear ($\alpha = 1$), the terms involving $\mathrm{VAR}[s]$ in Eq. (9) would drop out and a constant parameter α would suffice to preserve the average fluxes across scales.

(b) *Case of* $\lambda < \lambda_o$

For the case of applying the model at scales smaller than the one for which its parameterizations were optimized, the constraint to preserve the areal average flux becomes

$$s_{\lambda_o,i}^{\alpha_{\lambda_o}} = \langle s_\lambda^{\alpha_{\lambda,i}} \rangle_{\lambda_o,i}. \quad (10)$$

Here, λ is again the model grid-size but the scale of parameter optimization λ_o corresponds to a scale larger than λ (see Fig. 1(b)). Similarly to Case (a), the constraint equation can be applied at each grid box i of size λ_o providing a spatial distribution of $\alpha_{\lambda,i}$ or alternatively an $\alpha_{\lambda,\mathrm{eff}}$ could be found by taking the expectation over the space–time domain of interest.

Eqs. (6)–(9) developed under the case of $\lambda > \lambda_o$ apply to the case of $\lambda < \lambda_o$ in the same way. The only difference between the two cases is that in Case (a) λ_o is a subgrid scale and in Case (b) λ_o is an aggregation scale, relative to the model grid-size λ. It is important to emphasize that the variance of soil moisture within a box of a particular fixed size depends on the (subgrid-) scale at which observations are available and that for a particular fixed scale of observations the variance of soil moisture depends on the box size within which the process is considered. It is the interplay of these two scales that contributes to the conceptual differences between the cases of $\lambda > \lambda_o$ and $\lambda < \lambda_o$. In the following section, we will explore the variance of soil moisture as a function of (i) box size for a fixed scale of observations, and (ii) scale of observations for a fixed box size.

Then, we will connect these variances to the cases of interest, i.e., $\lambda > \lambda_o$ and $\lambda < \lambda_o$.

2.2. Dependence of soil moisture variability on scale of observations and model grid-size

Fig. 2 shows the spatial variability of relative soil moisture (top 5 cm of soil) derived from Electronically Scanned Thinned Array Radiometer (ESTAR) images during SGP97 at the scale of 0.8 km within an area of 51.2 km × 51.2 km. The solid white lines mark potential box sizes within which one might need to consider the spatial variability of soil moisture. Using this type of soil moisture fields from the SGP97 experiment, computations were performed to characterize the soil moisture variability with respect to the scale of observation and the size of the box within which the observations were considered. Before the computations are presented in Section 3, a conceptual analysis and intuitive explanation of the variability are given in this section.

First, fixing the scale of observations to say λ_1 (e.g., the highest resolution of 0.8 km for the SGP97 ESTAR) the box size was expanded from λ_1 to larger values

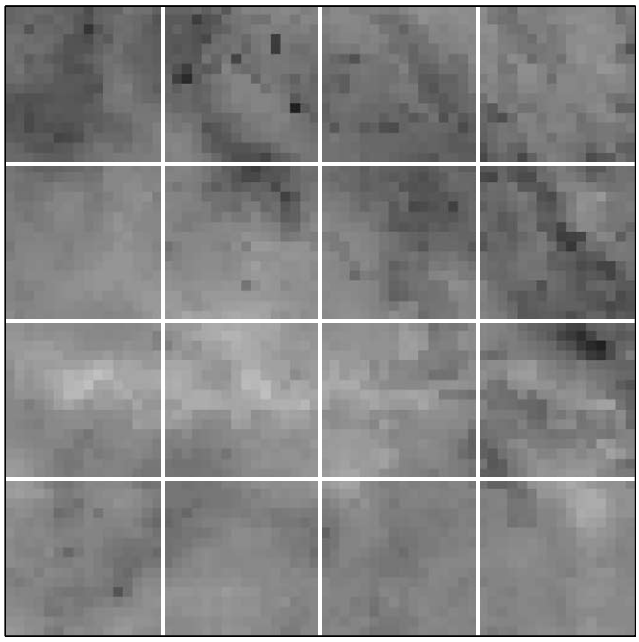

Fig. 2. Spatial variability of relative soil moisture derived from ESTAR during SGP97 within a 51.2 km × 51.2 km area for observational scale (pixel size) of 0.8 km. The solid white lines mark potential boxes within which the variability of soil moisture could be computed. By varying the observational scale (via aggregation of the finest resolution observations) and the size of the boxes, the curves of Fig. 3 can be computed.

$\lambda \geqslant \lambda_1$ and the variance of soil moisture as a function of box size was considered (see top curve in Fig. 3(a)). It is noted that for $\lambda = \lambda_1$ there is only a single observation pixel within each box (no variability) and the variance of the process within each box is therefore zero. As the box size increases to say $\lambda = 2\lambda_1$ (4 observation pixels within each box) or $\lambda = 4\lambda_1$ (16 observation pixels within each box) the variability of the process (always seen at the scale of observations λ_1) increases. It is noted that the variance is not computed from the 4 or 16 observations in a single box but, as explained later, conditional statistics are used to group together all boxes with equal average soil moisture and consider the within-box variability over the ensemble of boxes. By changing the scale of observations to say λ_2 or λ_3 (via aggregation of the fine resolution data) and repeating the above procedure, the other curves in Fig. 3(a) can be obtained.

Now consider the box size fixed, to say λ_x, and the scale of observations varying from λ_1 up to λ_x. Fig. 3(b) illustrates how the variability of soil moisture changes with the scale of observations for a fixed box size. As expected, the larger the scale of observations (aggregation level) the smaller the variance of soil moisture within areas of fixed size since aggregation smoothes out small-scale spatial heterogeneities. Notice that the curve of Fig. 3(b) can also be obtained as a special case of Fig. 3(a) by fixing the box size to a particular value (dashed vertical line).

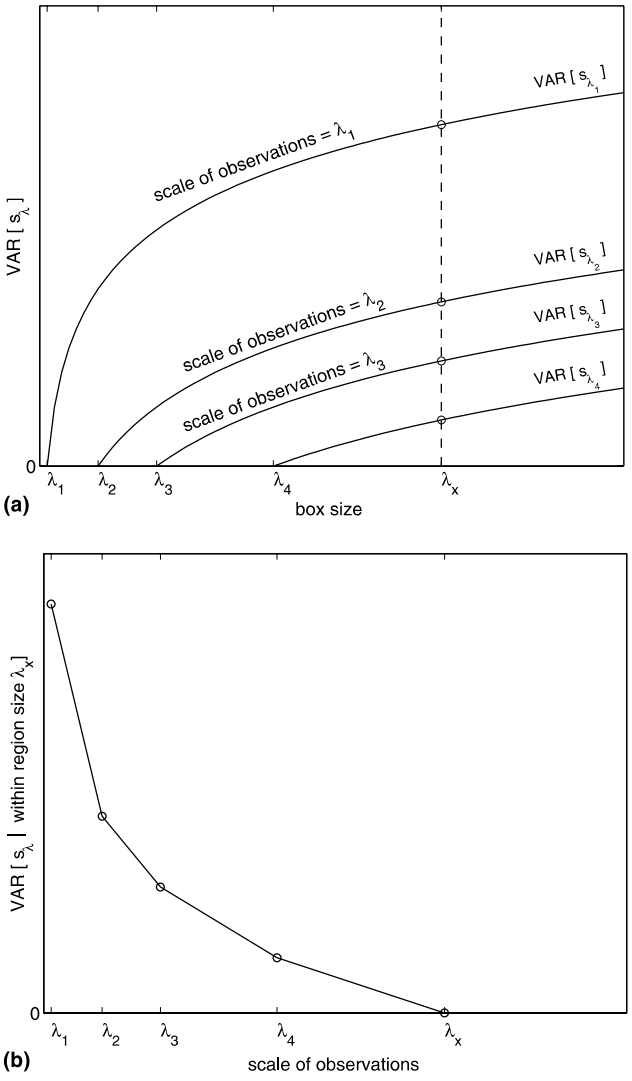

Fig. 3. Plot illustrating the dependence of soil moisture variability on scale. In the top plot, $\lambda_1, \lambda_2, \ldots$, etc. represent the scale at which observations are available. For any fixed scale of observations, as the box size increases from the scale of observations to a large area, the variability of the observations increases (top plot). For a particular box size, say λ_x, the variance of the process depends on the scale at which the process is seen, that is, the scale at which observations are available. The larger the scale of observations the smaller the variance of the process (bottom plot). Further explanation is provided in Section 2.

In the case of $\lambda > \lambda_o$, the "scale of observations" represents the scale of parameter optimization λ_o and the "box size" within which VAR$[s_{\lambda_o}]$ is computed is the model grid-size λ. The relevant variance as a function of scale corresponds to one of the curves in Fig. 3(a) where the x-axis would represent increasing model grid-size λ. In the case of $\lambda < \lambda_o$, the "box size" over which the variance of soil moisture is computed corresponds to the scale of parameter optimization λ_o and the "scale of observations" now relates to the grid-size λ at which a hydrologic or coupled model is run. This corresponds to Fig. 3(b) where VAR$[s_\lambda]$ is computed at different model

grid-scales λ within a fixed $\lambda_o \times \lambda_o$ area. The x-axis in this case would again represent increasing model grid-size.

2.3. Conditional statistics of soil moisture

There is evidence in the literature (e.g., [11,8,17]) to suggest that the spatial variability of soil moisture significantly depends on the mean soil moisture. Thus, the curves in Fig. 3 would better be described by conditioning the variance on the mean soil moisture, i.e., by considering the variability within boxes of the same box-averaged soil moisture value. In the solution of Eq. (9) for $\alpha_{\lambda,\text{eff}}$, we will acknowledge this dependency of the VAR$[s]$ on $E[s]$ by taking the expectation conditionally over a small range of $E[s]$ values and finding the $\alpha_{\lambda,\text{eff}}$ that applies to that $E[s]$ range.

In the conditional expectation for the case of $\lambda > \lambda_o$, grid boxes of size λ that have s_λ within a specified range of soil moisture values are grouped together as shown in Fig. 4. This conditional grouping can be performed by selecting boxes with similar s_λ over a spatial or space–time domain of interest. Note that the last term of Eq. (9) drops out when the expectation is taken over conditions of similar s_λ since the conditioning requires the s_λ values to be similar (at the limit the same value) and consequently makes the VAR$[s_\lambda]$ negligible. Eq. (9) then becomes

$$\lambda > \lambda_o : E[s_\lambda]^{\alpha_{\lambda,\text{eff}}} \cong E[s_{\lambda_o}]^{\alpha_{\lambda_o}} + \tfrac{1}{2}\text{VAR}[s_{\lambda_o}](\alpha_{\lambda_o}-1)\alpha_{\lambda_o}E[s_{\lambda_o}]^{(\alpha_{\lambda_o}-2)}. \quad (11)$$

The VAR$[s_{\lambda_o}]$ in Eq. (11) is the variance of soil moisture computed at the scale of parameter optimization λ_o and over the grouped $\lambda \times \lambda$ boxes with similar s_λ (i.e., a value obtained from one of the curves in Fig. 3(a) where the scale of observations is λ_o and the box size is λ). The expected value of the soil moisture is determined by the range of s_λ specified in the conditional grouping. This procedure of grouping together boxes of area $\lambda \times \lambda$ with similar s_λ creates a hypothetical domain of sufficient size such that the conditional variance of soil moisture will be independent of the domain size (for stationary fields) but dependent on the scale λ used to perform the conditional grouping.

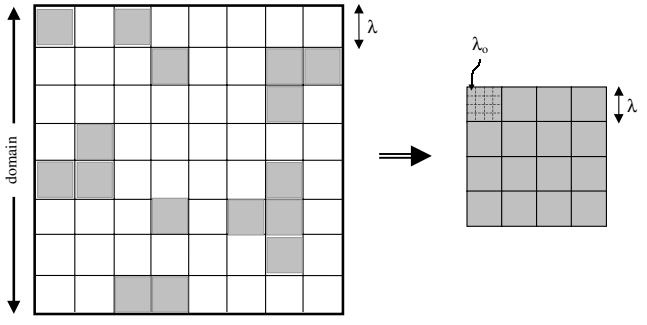

Fig. 4. Schematic of grouping together boxes of size λ with similar s_λ (gray shaded boxes) for conditional statistics in the case of $\lambda > \lambda_o$.

For the case of $\lambda < \lambda_o$, the conditional grouping would be performed by selecting boxes of size λ_o with similar s_{λ_o} over a desired space–time domain. In this case, conditional expectation for a specified s_{λ_o} range would result in a negligible conditional VAR$[s_{\lambda_o}]$ and the second term of Eq. (9) would drop out, resulting in

$$\lambda < \lambda_o : E[s_\lambda]^{\alpha_{\lambda,\text{eff}}} \cong E[s_{\lambda_o}]^{\alpha_{\lambda_o}} - \tfrac{1}{2}\text{VAR}[s_\lambda](\alpha_{\lambda,\text{eff}}-1)\alpha_{\lambda,\text{eff}}E[s_\lambda]^{(\alpha_{\lambda,\text{eff}}-2)}. \quad (12)$$

The VAR$[s_\lambda]$ in Eq. (12) is the variance of soil moisture at the model grid-size λ and computed over the $\lambda_o \times \lambda_o$ conditionally grouped boxes. That is, VAR$[s_\lambda]$ would correspond to a value obtained from the curve of Fig. 3(b) where the scale of observations is λ and the whole curve was obtained for a specified $E[s_{\lambda_o}]$ and by fixing the box size to the scale of parameter optimization λ_o.

2.4. Analytical dependence of nonlinear parameterizations on soil moisture variability

Having explored how VAR$[s_{\lambda_o}]$ and VAR$[s_\lambda]$ are computed for the cases of $\lambda > \lambda_o$ and $\lambda < \lambda_o$, respectively, we return to the original problem of exploring the scale-dependency of the parameter α_λ such that spatially averaged fluxes are preserved across scales. Hereafter, the parameter $\alpha_{\lambda,\text{eff}}$ will be abbreviated to α_λ. We start from Eqs. (11) and (12) which are conditioned on the larger-scale mean soil moisture and try to analytically compute the value of α_λ as a function of the mean and variance of soil moisture. For illustration purposes we assume the value of $\alpha_{\lambda_o} = 4$ as, for example, used in the surface runoff parameterization of BATS for non-frozen soil ([5]; also see Appendix A). To get insight into the differences between the values of α_λ and α_{λ_o}, and more generally on the scale-dependency of α, some analytical solutions are shown in Fig. 5.

The case of $\lambda > \lambda_o$ (i.e., model grid-size λ larger than the scale λ_o of parameter optimization), is shown in Fig. 5(a). The curves correspond to analytical solutions of Eq. (11) for α_λ as a function of VAR$[s_{\lambda_o}]$ for several different mean soil moisture conditions. Similarly, Fig. 5(b) shows the analytical solution of Eq. (12) which corresponds to the case of $\lambda < \lambda_o$ (i.e., model grid-size smaller than the scale of parameter optimization). Figs. 5(a) and (b) illustrate that the difference between the fixed value α_{λ_o} (here assumed equal to 4) at the scale of parameter optimization and the scale-dependent value α_λ increases with increasing variance of the soil moisture. Moreover, the rate of deviation of α_λ from α_{λ_o} as a function of soil moisture variability also depends on the mean soil moisture level, with the larger deviations being observed at the extreme (both the low and high ends)

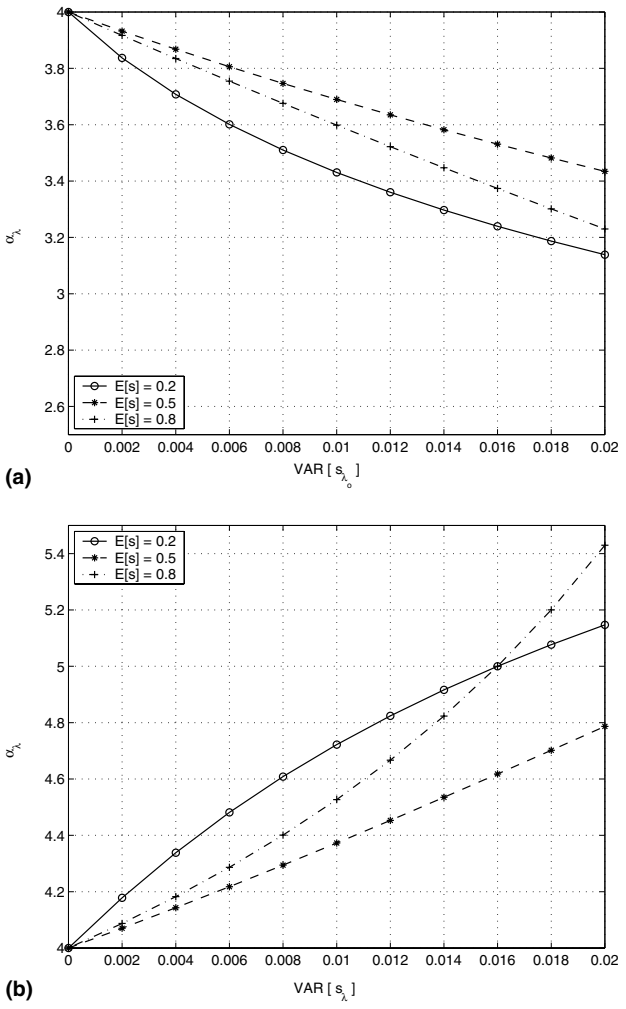

Fig. 5. Analytically derived α_λ as a function of mean and variance of soil moisture for (a) $\lambda > \lambda_o$ and (b) $\lambda < \lambda_o$. At $\lambda = \lambda_o$ the parameter value was set to 4 (a typical value for runoff production). Notice that if the model is applied at scale λ which is larger than λ_o then the parameter α_λ decreases in value. Conversely, if the model is applied at scale λ which is smaller than the scale λ_o at which the parameterization was optimized, then the parameter α_λ increases in value.

mean soil moisture levels. For a fixed soil moisture range and variability, the value of α_λ needed to preserve fluxes across scales becomes less than 4 in the case of $\lambda > \lambda_o$ and greater than 4 in the case of $\lambda < \lambda_o$. In the following section, we use SGP97 airborne remotely sensed soil moisture data to quantify how $\mathrm{VAR}[s_{\lambda_o}]$ and $\mathrm{VAR}[s_\lambda]$ change with scale such that the dependency of α_λ on scale can be consequently quantified.

3. Soil moisture variability and its scale-dependency

3.1. SGP97 ESTAR derived soil moisture

The scale-dependency of nonlinear parameterizations involving soil moisture was shown in the previous section to be theoretically related to the scale-dependency of the variance of soil moisture. Rodriguez-Iturbe et al. [17] found that the variance of soil moisture in the top 5 cm of soil follows a power law decay as a function of increasing scale. Their findings were based on statistical analysis of in situ soil moisture measurements and 200 m resolution soil moisture data retrieved from Electronically Scanned Thinned Array Radiometer (ESTAR) images during the Washita '92 Experiment which covered an area of 18 km × 45 km in southwest Oklahoma (see [12] for details on the Washita '92 experiment). Rodriguez-Iturbe et al. [17] found that this power law decay held for scales ranging from 30 m up to 1 km and that the slope of the log–log plot of the variance versus scale was dependent on the average soil moisture conditions. Hu et al. [11] found that the scaling relationship of Rodriguez-Iturbe et al. [17] could be extended up to scales of 4.4 km for the Washita '92 ESTAR derived soil moisture data.

The Southern Great Plains Hydrology Experiment in June 18–July 18, 1997 (SGP97) provided an additional source of observed high resolution soil moisture data. The SGP97 Hydrology Experiment was a field campaign covering south central Kansas and most of central Oklahoma. Intensive field observations were collected, quality controlled and cross calibrated and validated. During SGP97, ESTAR was used to map soil moisture. Data were collected over a strip of approximately 50 km (West–East) by 250 km (North–South) at a 0.8 km ground resolution. Details on the algorithm used for converting ESTAR images to soil moisture, data processing, and verification can be found in [12,13]. The reader is referred to daac.gsfc.nasa.gov/CAMPAIGN/DOCS/SGP97/sgp97.html for a detailed description of the SGP97 experiment and information on where to obtain the soil moisture data.

The SGP97 ESTAR derived soil moisture data were used in this study to quantify how the variance of soil moisture in the upper layer of soil (top 5 cm) changes with scale. The soil moisture data mapped by the ESTAR are volumetric soil moisture in absolute percent, i.e., percent of the 0.8 km × 0.8 km × 5 cm volume of soil that is occupied by water. In order to obtain the relative soil moisture, these values were divided by the spatially variable porosity field of the soil co-located with the SGP97 ESTAR region. The relative soil moisture within the 0–5 cm surface layer is hereafter denoted as s and the volumetric soil moisture as w.

Fig. 2 serves as an illustration of the pronounced spatial variability of soil moisture observed during the SGP97. The soil moisture data were aggregated from the original 0.8 km ESTAR data to obtain fields at coarser resolutions. An extensive analysis of the frequency histograms of soil moisture for different aggregation levels and different average wetness conditions can be found in [15] but are not reproduced here for brevity.

3.2. Scale-dependency of SGP97 soil moisture variability

As discussed before, there are two ways pertinent to our study to look at how the variability of soil moisture changes with scale. One approach is to fix the resolution of the data at the resolution of the ESTAR instrument of 0.8 km and follow how the variance of the soil moisture changes with increasing area of consideration or model grid-size (see Fig. 3(a)). The other way is to specify a fixed area of interest, aggregate the data within that area, and follow how the variance of the soil moisture changes with aggregation level (see Fig. 3(b)). The first case corresponds to the situation at which the grid-size of the model λ is larger than the scale of parameter optimization λ_o and thus the interest lies on determining the effect of within-pixel variability (not seen by the model) on fluxes or parameter values at scale λ relative to the initial values at scale λ_o. The second case corresponds to the situation at which the grid-size of the model λ is smaller than the scale of parameter optimization λ_o and thus the interest lies on determining the effect of the small-scale variability (not accounted for in the parameter optimization which occurred at a larger scale) on fluxes or parameter values at scale λ relative to the initial values at scale λ_o.

For the case of $\lambda > \lambda_o$, the SGP97 region was subdivided into $\lambda \times \lambda$ size boxes. In this case, λ_o was fixed at 0.8 km and the scale λ (representing the scale at which the model would run) was changed from 1.6 to 51.2 km. Fig. 6(a) shows the SGP97 region subdivided into boxes of $\lambda = 12.8$ km. For the case of $\lambda < \lambda_o$, the scale λ_o was fixed at the 51.2 km approximate width of the SGP97 region and the scale λ was varied from 0.8 to 25.6 km. Here, the scale λ represents aggregating the ESTAR derived soil moisture data to coarser scales. The SGP97 region was subdivided into five boxes of size 51.2 km × 51.2 km as shown in Fig. 6(b). In both cases, boxes over the selected space–time domain (here the spatial domain of SGP97 was considered for each of the 16 days with available ESTAR images; one image per day) were grouped according to the average relative soil moisture ($E[s]$) and conditional statistics were computed over the grouped boxes (see Fig. 4). Boxes with missing data were discarded and variances were only computed for scales and average soil moisture groupings with 30 or more values for meaningful statistics.

The scale-dependency of the spatial variability of the SGP97 soil moisture data is shown in Fig. 7. For the case of $\lambda > \lambda_o$, when the scale of observations is fixed at $\lambda_o = 0.8$ km the VAR$[s_{\lambda_o}]$ was found, as expected, to increase with the box size within which the data were considered (i.e., model grid-size λ) as shown in Fig. 7(a). The magnitude of the variance as a function of scale was also found to depend on the average relative soil moisture and to be higher as the average soil conditions became more wet. For the case of $\lambda < \lambda_o$,

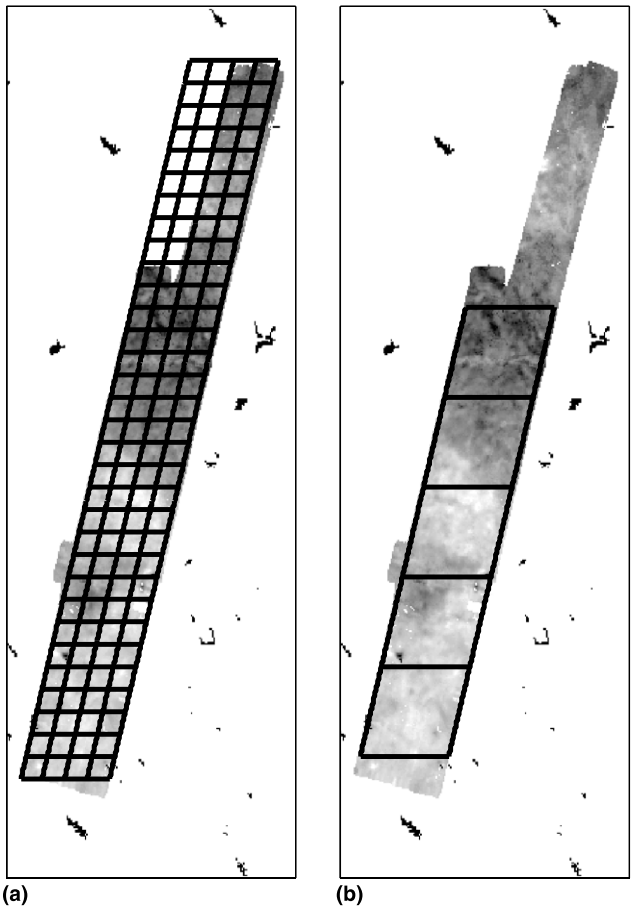

Fig. 6. (a) For $\lambda > \lambda_o$, we fixed λ_o (the scale for which the parameterization was optimized) at 0.8 km and computed the VAR$[s_{\lambda_o}]$ within boxes of size $\lambda \times \lambda$, where λ is the scale at which the model would run. The VAR$[s_{\lambda_o}]$ is shown in Fig. 7(a). The scale λ was varied from 1.6 to 51.2 km. Here the boxes of $\lambda = 12.8$ km are shown. (b) For $\lambda < \lambda_o$, we fixed λ_o (the scale for which the parameterization was optimized) at 51.2 km and computed the VAR$[s_\lambda]$ within $\lambda_o \times \lambda_o$ size boxes where λ represents the scale at which the model would run (and therefore at which the variability of the soil moisture field would be seen by the model). The VAR$[s_\lambda]$ is shown in Fig. 7(b). The scale λ was varied by aggregating the soil moisture data from the ESTAR resolution of 0.8 km up to 25.6 km. As shown here, five $\lambda_o \times \lambda_o$ boxes fit within the SGP97 region. In both cases (a) and (b), boxes with missing data were discarded from the variance computation. The west and east sides of the boxes were aligned parallel to the NASA P-3 aircraft flight lines.

Fig. 7(b) shows how the variance of the relative soil moisture changes with aggregation scale λ within a fixed box size of $\lambda_o = 51.2$ km. Variances for scales larger than 25 km are not shown in Fig. 7(b) since there were not enough data points at the larger scales to compute a meaningful variance. Our results indicate that the trend of how the magnitude of the variance changes with the average relative soil moisture might not always be monotonic, i.e., an increase in average soil moisture does not necessarily imply an increase in VAR$[s_\lambda]$ (see Fig. 7(b)). In fact, the range of $E[s] = 0.4$

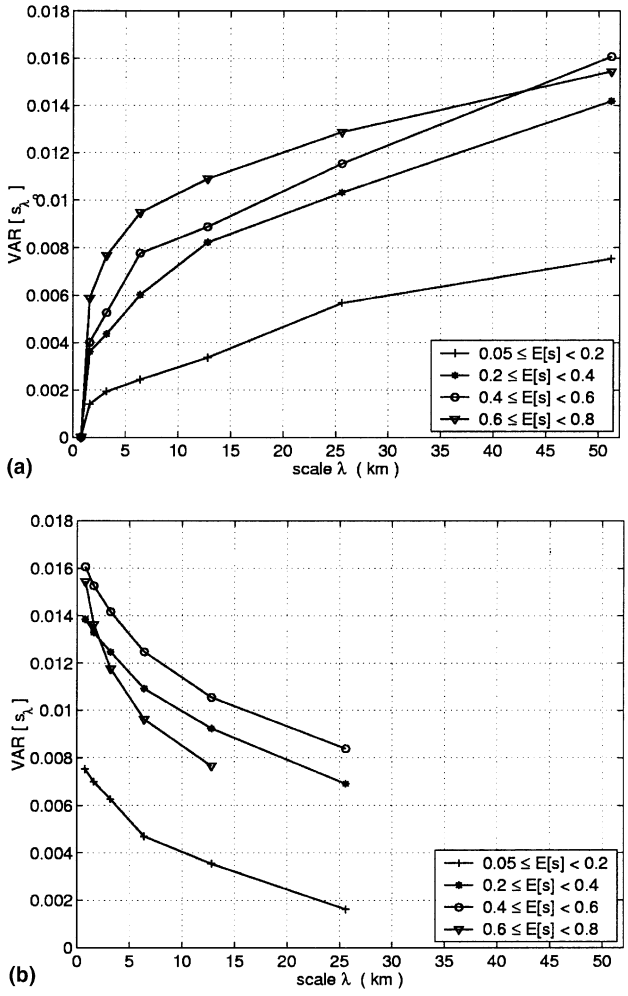

Fig. 7. Scale-dependency of the variance of soil moisture for (a) the case when the scale λ_o at which the parameterization was optimized is smaller (and here fixed to 0.8 km) than the model grid-size λ and (b) the case when the scale λ_o at which the parameterization was optimized is larger (and here fixed to 51.2 km) than the model grid-size λ.

to 0.6 shows the highest spatial variability at all scales, while the range 0.6–0.8 was found to have the most drastic scale-dependency (i.e., faster rate of change in magnitude of the variance with scale). As expected, Fig. 7(b) shows that the variance of soil moisture decreases as the scale increases.

3.3. Scaling of soil moisture variance

The log–log plot of variance of relative soil moisture versus scale found by Rodriguez-Iturbe et al. [17] for Washita '92 data is shown in Fig. 8(a) along with the curves found in this study for the SGP97 data. This figure shows a potential scaling break at the intersection of the scales of the two experiments. This break in scaling could be caused by several different factors. One possible reason is that there could truly be a scaling break at scales of 1 km^2 switching from a log–log linear relationship to nonlinear. Another possible reason for the scaling break could be the difference between the Washita '92 being a drydown period and SGP97 being a period of frequent rainfall. Hu et al. [11] found that the scaling relationship of Rodriguez-Iturbe et al. [17] is valid over a wider range of scales. However, they were using volumetric soil moisture rather than relative soil moisture. In order to compare with Hu et al. [11], the variance of the SGP97 volumetric soil moisture data was computed using 51.2 km × 51.2 km boxes shown in Fig. 6(b) and aggregating the data inside the boxes. The boxes were grouped according to the average soil moisture and the conditional variance was computed for each aggregation scale and volumetric soil moisture class with more than 30 data points. Fig. 8(b) shows the Washita '92 data of Hu et al. [11] along with the SGP97 data. The lack of agreement between the Washita '92 and SGP97 data suggests that the soil moisture fields do not exhibit scaling under all conditions and at all scales.

In order to test if the scaling break can be explained by the differing rainfall conditions between SGP97 and Washita '92, a 3-day period of drydown conditions during SGP97 which occurred on July 1–3, 1997 in the uppermost 51.2 km × 51.2 km box of Fig. 6(b) was used to reassess the scaling relationships. The conditional statistics procedure of grouping together boxes over the space–time domain of similar average soil moisture conditions was not used for the drydown period comparison. Rather, the same technique as used by Rodriguez-Iturbe et al. [17] and Hu et al. [11] of aggregating soil moisture data inside one specified region and computing the variance for each aggregation scale was used for the SGP97 drydown period data. Fig. 9(a) shows the log–log plot of variance of relative soil moisture versus scale ($\lambda \times \lambda$ resolution of the data) for the drydown period of the subregion of SGP97 with that of Rodriguez-Iturbe et al. [17]. Fig. 9(b) shows a similar log–log plot for the volumetric soil moisture of the drydown period of the SGP97 subregion with that of Hu et al. [11]. It can be seen from Fig. 9 that the scaling break between SGP97 and Washita '92 is not the result of differing rainfall conditions since it still occurs when only drydown periods were considered. Furthermore, it illustrates that the scaling break found in this study is not an artifact of the conditional statistics approach since now the same processing procedure used by Rodriguez-Iturbe et al. [17] and Hu et al. [11] on the Washita '92 soil moisture data was also used on the SGP97 data shown in Fig. 9. In fact, our processing algorithms applied to the Washita '92 volumetric soil moisture data (available at hydrolab.arsusda.gov/washita92/wash92.htm) reproduced the log–log linear relationship reported in [11] (see Fig. 10). These discrepancies and the question as to whether or not, or under what conditions, soil moisture fields exhibit sim-

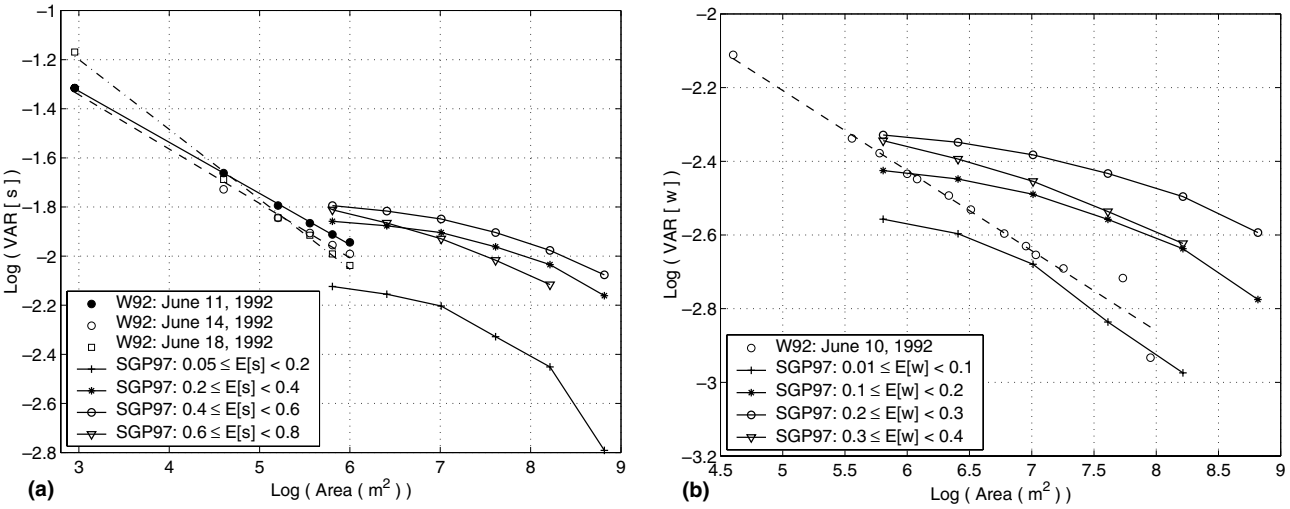

Fig. 8. (a) Superposition of findings of Rodriguez-Iturbe et al. [17] where a log–log linear relationship of VAR[s] with scale was found from Washita '92 relative soil moisture data between scales of 30 m and 1 km and our findings where lack of simple scaling is found from the SGP97 relative soil moisture data over scales of 0.8–25.6 km. (b) Superposition of findings of Hu et al. [11] where a log–log linear relationship of VAR[s] with scale was found from Washita '92 volumetric soil moisture data between scales of 200 m and 4.4 km and our findings where lack of simple scaling is found from the SGP97 volumetric soil moisture data over scales of 0.8–25.6 km. Here, area refers to the $\lambda \times \lambda$ scale of the data.

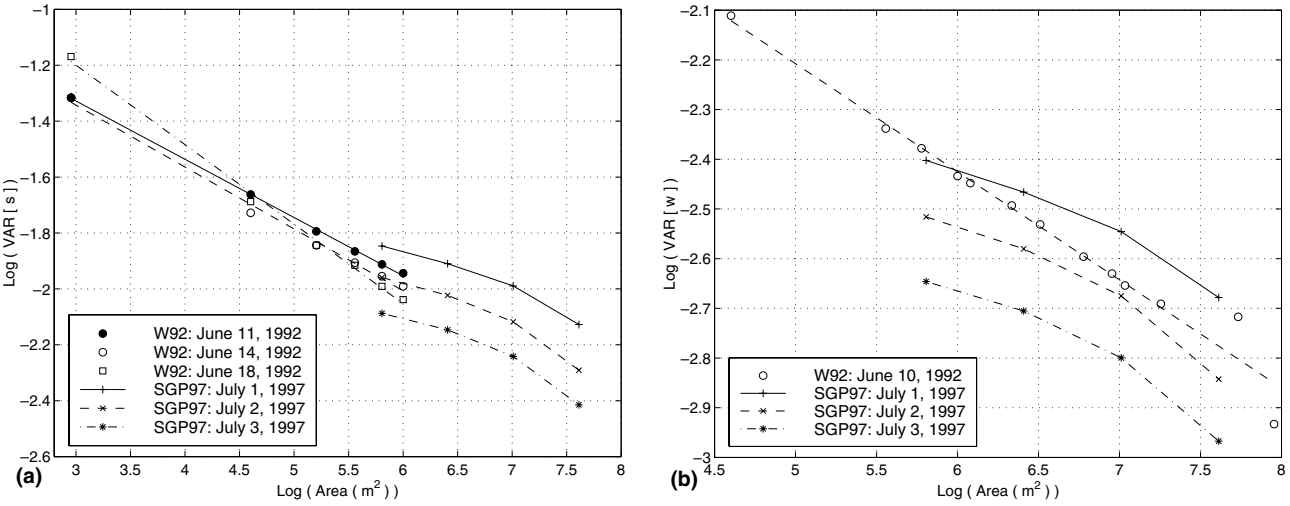

Fig. 9. Log–log plot of the variability of soil moisture versus area during drydown conditions characterized by a period of no rainfall for (a) SGP97 relative soil moisture at scales 0.8–6.4 km superimposed with the results of Rodriguez-Iturbe et al. [17] Washita '92 relative soil moisture at scales 30 m to 1 km and (b) SGP97 volumetric soil moisture at scales 0.8–6.4 km superimposed with the results of Hu et al. [11] Washita '92 volumetric soil moisture at scales 200 m to 4.4 km. The uppermost box shown in Fig. 6(b) was used for the SGP97 soil moisture data.

ple scaling need to be further examined but fall beyond the scope of this study.

4. Scale-dependency of nonlinear parameterization

Combining the scale-dependency of the SGP97 relative soil moisture shown in Figs. 7(a) and (b) with Eqs. (11) and (12), the scale-dependency of the parameter α of nonlinear relationships of the form $F \sim s^{\alpha}$ involving soil moisture can be computed. Fig. 11 shows the spatial distribution of α_λ values for one 51.2 km $\times$ 51.2 km area with a 0.6 average relative soil moisture. The parameter α_λ was computed by solving the constraint equation (4) at each $\lambda \times \lambda$ box and assuming $\alpha_{\lambda_o} = 4$, a typical value used in runoff production. In this case, the scale λ_o for which the parameterization was optimized was fixed at 0.8 km and the scale λ was varied from 1.6 to 51.2 km (i.e., $\lambda > \lambda_o$) as shown in Fig. 11(a)–(c). The cumulative frequency of α_λ computed from an ensemble of 51.2 km $\times$ 51.2 km areas (over the SGP97 space–time domain) with average relative soil moisture in the range 0.6–0.8 and for selected spatial resolutions of 1.6, 3.2, 6.4, and 12.8 km are shown in Fig. 12. It is interesting to

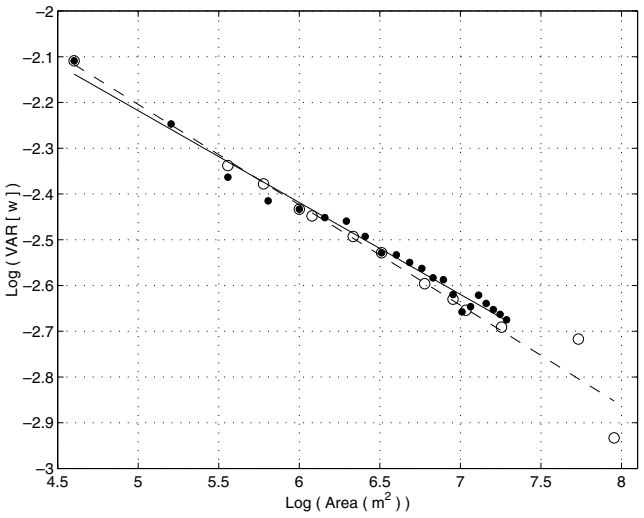

Fig. 10. Log–log plot of the variability of soil moisture versus area for the Washita '92 volumetric soil moisture data on June 10, 1992. The open circles and dashed line linear fit correspond to the results of Hu et al. [11]. The filled circles and solid line linear fit correspond to the results found in this study. The agreement between the two sets of results provides evidence that the lack of simple scaling found in this study for the SGP97 soil moisture data is not an artifact of our processing procedure.

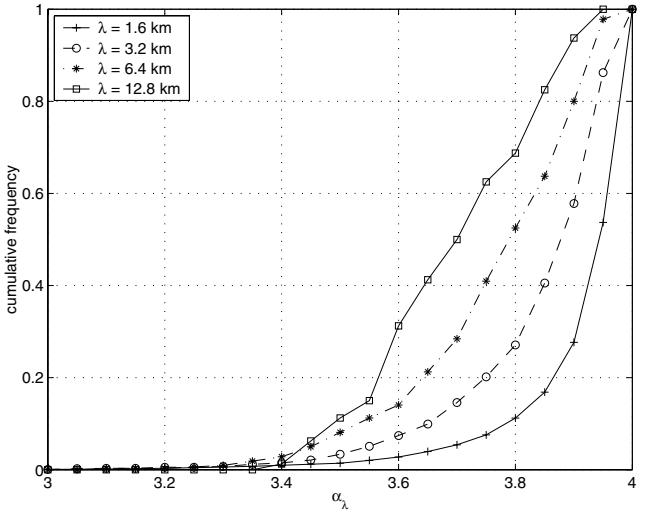

Fig. 12. Cumulative frequency of the spatially distributed α_λ parameter values computed from an ensemble of 51.2 km × 51.2 km areas with average relative soil moisture in the range of 0.6–0.8. Recall that $\alpha_{\lambda_o} = 4$ is the value that preserved the fluxes when the scale λ was equal to the optimization scale λ_o (here assumed to be the 0.8 km resolution of the ESTAR derived soil moisture).

observe that the values of α_λ needed to preserve the box-by-box fluxes have a considerable variability from the fixed value of $\alpha_{\lambda_o} = 4$ which is typically applied to all boxes if scale-dependency is ignored.

When one considers preservation of fluxes on the average over all boxes of the space–time domain of interest, an effective parameter α_λ results which is computed by solving Eqs. (11) and (12) for the cases of $\lambda > \lambda_o$ and $\lambda < \lambda_o$ as is shown in Figs. 13(a) and (b), respectively. (Note that the so-computed effective value of α_λ is not necessarily equal to the arithmetic average of the spatially variable α_λ values computed above due to nonlinearities.) As the scale λ (at which the model is run) deviates from λ_o (the scale at which the parameterization was optimized), the value of α_λ needed to preserve the average fluxes also deviates from α_{λ_o}. For $\lambda > \lambda_o$, this corresponds to $|\alpha_\lambda - \alpha_{\lambda_o}|$ increasing with increasing scale. When $\lambda < \lambda_o$, $|\alpha_\lambda - \alpha_{\lambda_o}|$ increases with decreasing scale. Moreover, the spread of the lines shown in Fig. 13 demonstrates the strong dependency of the variance of soil moisture and, consequently, α_λ on the average soil moisture conditions.

To get insight as to the significance of the difference in considering $\alpha = 4$ versus $\alpha = 4.2$ on the computed fluxes, we concentrate on the $R_s = s^\alpha G$ relationship used in BATS and discussed in more detail in Appendix A. In this relationship, the flux R_s is surface runoff, s is the arithmetic average of the relative soil moisture in the 10

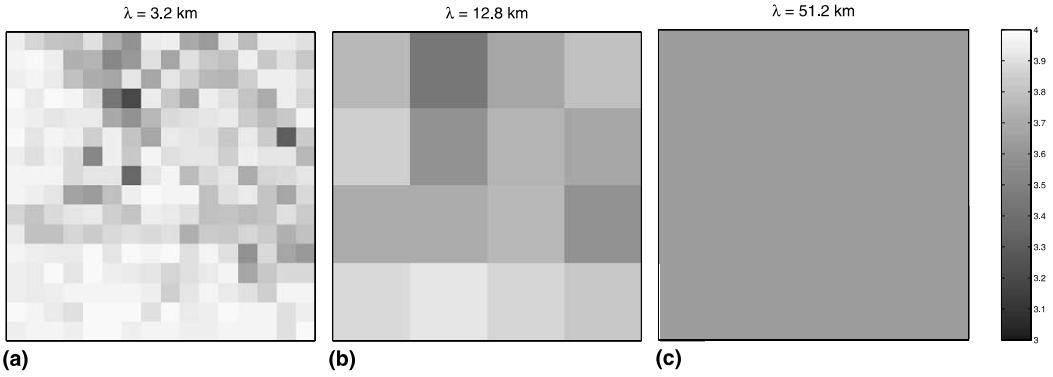

Fig. 11. Spatial distribution of the parameter α_λ for the case of $\lambda > \lambda_o$ where $\lambda_o = 0.8$ km and $\alpha_{\lambda_o} = 4$. The 51.2 km × 51.2 km box shown has a 0.6 average relative soil moisture. Notice that if a single parameter α was to be used for the entire grid of 51.2 km then a value of $\alpha = 3.6$ and not $\alpha = 4$ would be needed to preserve the fluxes at the 51.2 km scale. If the grid size of the model was 25.6 km notice the spatial variability of soil moisture would determine the spatial variability of the appropriate value of α_λ for box-by-box flux preservation.

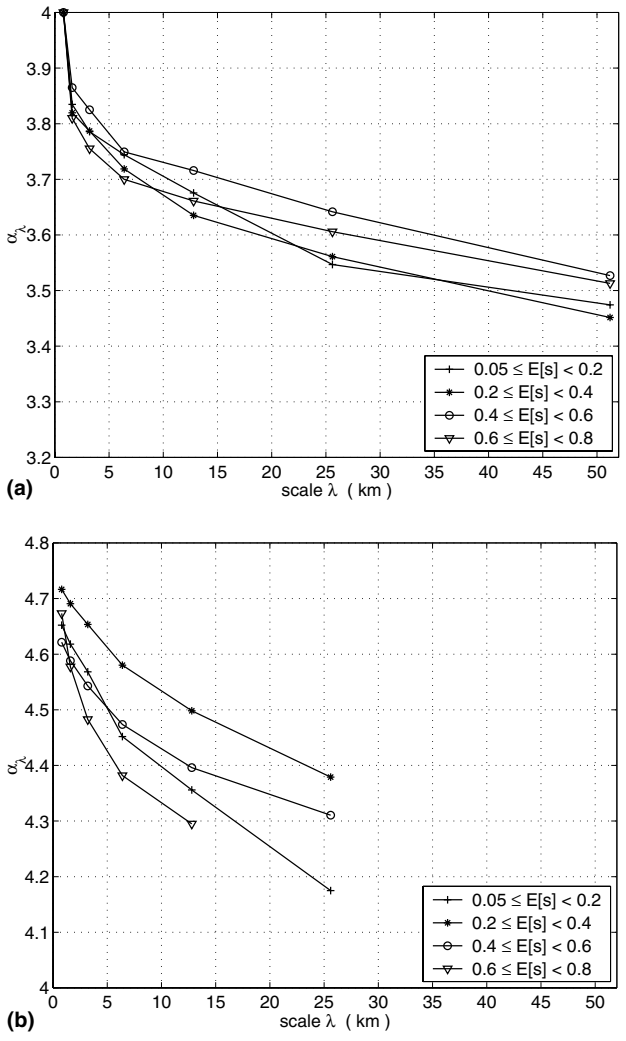

Fig. 13. Scale-dependency of the parameter α_λ for (a) the case when the scale λ_o at which the parameterization was optimized is smaller than the model grid-size λ and (b) the case when the scale λ_o at which the parameterization was optimized is larger than the model grid-size λ. Recall that $\alpha_{\lambda_o} = 4$.

cm surface layer and the 100 cm root zone layer, and G is the net input of water to the soil surface. As discussed in Appendix A, the BATS surface runoff parameterization was developed for climate scales but is often applied at smaller scales. This corresponds to the case of $\lambda < \lambda_o$ which is shown schematically in Fig. 1(b) and analytically in Fig. 5(b). The percent changes in surface runoff R_s produced by keeping the same G and using $\alpha = 4$ versus the values of α_λ for different VAR$[s]$ and $E[s]$ values (see Fig. 5(b)) are shown in Fig. 14. Using $\alpha = 4$ instead of $\alpha = 4.4$, for example, results in a significant overestimation (ranging from 10% to 50%, depending on the average relative soil moisture) of the surface runoff. It was shown in Fig. 13(b) that, for the case of $\lambda < \lambda_o$, the α_λ parameter increases as the scale decreases. Although the relative soil moisture data used in Fig. 13(b) represent the top 5 cm of soil, it is expected that

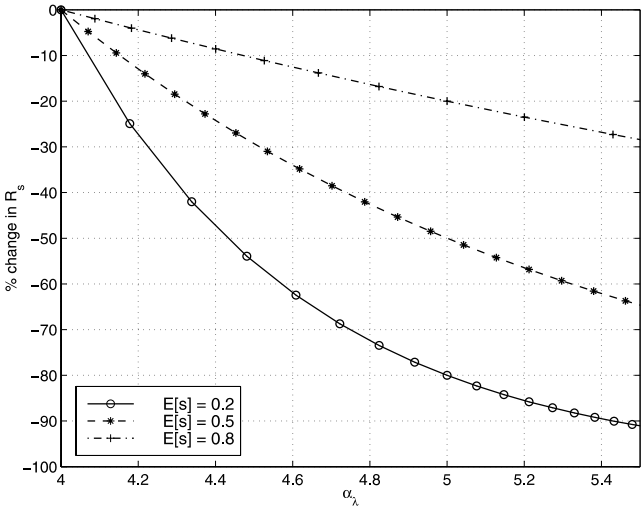

Fig. 14. Percent change in surface runoff produced by keeping the net input of water to the soil surface the same and using $\alpha = 4$ versus the VAR$[s]$ and $E[s]$ dependent α parameter values (see Fig. 5(b)) in the $R_s = s^\alpha G$ relationship of BATS.

the trend would be similar for the weighted average relative soil moisture variable used in the BATS surface runoff parameterization. In other words, as the model grid-size decreases from the 50–100 km climate scale of parameter optimization to much smaller model grid-sizes used today, the systematic bias introduced in the surface runoff prediction becomes very significant. Even if the value of the surface runoff is not important to a particular application (e.g., not concerned with streamflow prediction), the accuracy of the surface runoff must still

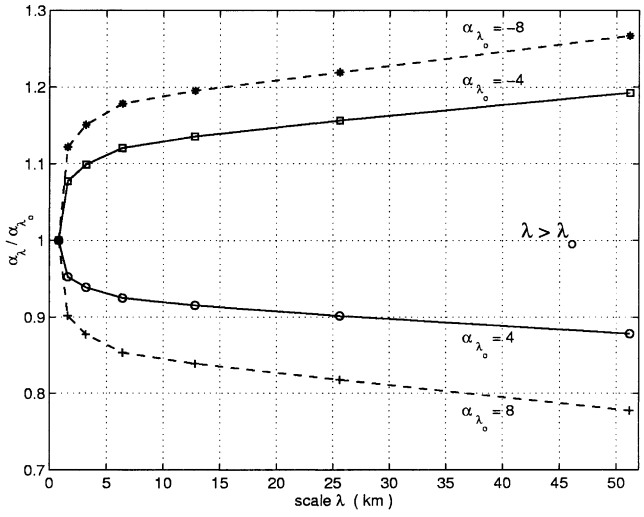

Fig. 15. Sensitivity of the scale-dependency of α_λ to the degree of nonlinearity of the parameterization (value of α_{λ_o}) for the range $0.6 \leqslant E[s] < 0.8$ and when the scale λ_o at which the parameterization was optimized is smaller than the model grid-size λ. Note that for a fixed scale λ, the deviation of the "relative bias factor" $\alpha_\lambda/\alpha_{\lambda_o}$ from unity increases as the nonlinearity of the relationship (i.e., $|\alpha_{\lambda_o}|$) increases.

be considered since it effects the soil moisture through the water balance and, consequently, the surface temperature and latent and sensible heat fluxes through the energy balance. Moreover, as has been demonstrated by other studies (e.g., [16]) these biases over small scales may grow nonlinearly over time and create larger-scale biases in the predicted fluxes.

As previously discussed, the scale-dependency of α is affected by both the spatial variability of soil moisture and the degree of nonlinearity of the relationship, i.e., the specific value of α_{λ_o}. Fig. 15 shows the "relative bias factor" $\alpha_\lambda/\alpha_{\lambda_o}$ which depicts the effects of changing α_{λ_o} on the scale-dependency of α_λ for positive and negative values of α_{λ_o}. The larger the nonlinearity of the relationship (e.g., $\alpha_{\lambda_o} = 8$ or -8), the larger the effects of scale on the parameter value. This explains theoretically why other studies have stated that the sensitivity of predicted fluxes to spatial variability is different for different models (e.g., [9,14]; among others).

5. Summary and conclusions

In this study, the scale-dependency of parameterizations which are nonlinear functions of variables exhibiting considerable spatial variability across a wide range of scales was examined. The motivation of the study was the fact that the scales at which hydrologic or coupled atmospheric–hydrologic models are run are often different from the scales at which the model parameterizations were optimized. If the parameterizations are kept the same, as is typically done, this discrepancy in scales can cause significant biases in the computed fluxes as has been documented by other studies. Alternatively, if fluxes were to be preserved at a specific scale of interest, the parameterizations could be modified accordingly to account for the discrepancy in scales. This second approach was adopted in this study and using an analytical methodology the dependence of the parameters on scale and the spatial variability of the involved variables was documented. For illustration purposes we focused on parameterizations which are explicit nonlinear functions of soil moisture and have the general form $F \sim s^\alpha$ where F is a predicted flux, s is soil moisture, and α is a parameter. The parameterization was assumed to keep the same form at all scales and the parameter α needed to preserve the areal average flux at various scales was quantified in terms of the scale-dependent variability of soil moisture. The SGP97 ESTAR derived data were used to characterize the spatial variability of soil moisture.

Denoting by α_{λ_o} the value of α at the scale λ_o at which the parameterization was optimized and by α_λ the value of α at the scale at λ which the model is run, explicit expressions of α_λ were derived as functions of scale, the value of α_{λ_o}, the average soil moisture state, and the spatial variability of the soil moisture field. It was found that the deviation of α_λ from α_{λ_o} increased as the discrepancy between scale λ and λ_o increased, as the degree of nonlinearity increased, and as the spatial variability of the soil moisture field increased. Also, the scale-dependency of α was higher for the extreme (both the low and high ends) of mean soil moisture levels.

The results of this study emphasize that if modifications are not made to nonlinear parameterizations to account for the mismatch between the scale for which they were developed and the scale at which they are applied, systematic biases may result in model-predicted water and energy fluxes. An example involving surface runoff predictions was used to illustrate the significant magnitude of these biases. Our study also provides a framework by which one can obtain how parameters of nonlinear relationships might be modified to account for the change in scale based on characterization of the spatial variability of soil moisture.

An integral part of this study was to examine in detail how the statistical moments of soil moisture (both relative and volumetric soil moisture representative of the 0–5 cm surface layer) depend on scale both for drydown periods (no rainfall) and periods of rainfall activity. It was found that our results did not quite agree with the results of Rodriguez-Iturbe et al. [17] and Hu et al. [11] who have reported log–log linear relationships of the variance of soil moisture with scale (simple scaling). Some reasons for this discrepancy have been offered, but they point out to the necessity to further examine these relationships over a wider range of scales, under different wetting conditions, and with observations from different sensors.

Acknowledgements

This work has been supported by the joint NOAA/NASA GCIP program under a NASA grant NAG8-1519. The first author gratefully acknowledges the support of a USDA National Needs Fellowship in Water Science. Computer resources were kindly provided to us by the Minnesota Supercomputing Institute. The authors thank the SGP97 participants for collecting and processing the ESTAR derived soil moisture data and making it readily available to the research community.

Appendix A. Surface runoff parameterization of BATS

The surface runoff parameterization used in the Biosphere–Atmosphere Transfer Scheme (BATS) (see [5] for details) follows the general form of a nonlinear power law relationship given by Eq. (1). At each model grid box, the surface runoff is computed according to

$$R_s = s^\alpha G, \tag{A.1}$$

where R_s is the surface runoff, s is the arithmetic average of the relative soil moisture in the 10 cm surface layer and the 100 cm root zone layer, $\alpha = 4$ for unfrozen soil, and G is the net input of water to the soil surface computed as the precipitation minus evaporation plus snow melt. Both s and G are variables that exhibit considerable spatial variability across a wide range of scales. It will be shown here that multiplication of the right-hand side of Eq. (2) by a variable which also has a scale-dependency does not alter the resulting equation (9).

Yang and Dickinson [20] explain that the BATS surface runoff parameterization was developed for climate scale (i.e., $\lambda_o = 50$ to 100 km) and parameterized to predict, on the average, similar surface runoff as is observed at those scales. As inexpensive, powerful computing resources become more readily available, the BATS land surface model is being run at spatial scales smaller than those for which its surface runoff parameterization was intended. This corresponds to the case of $\lambda < \lambda_o$ (see Fig. 1(b)). The constraint equation to preserve the λ_o scale surface runoff flux is

$$s_{\lambda_o,i}^{\alpha_{\lambda_o}} G_{\lambda_o} = \langle s_{\lambda}^{\alpha_{\lambda,i}} G_{\lambda} \rangle_{\lambda_o,i}. \tag{A.2}$$

Following the discussion in Section 2.1, a spatial distribution of $\alpha_{\lambda,i}$ could be found by applying the constraint equation given above at each grid box i of size λ_o or alternatively an $\alpha_{\lambda,\mathrm{eff}}$ could be found by taking the expectation over the space–time domain of interest

$$E[s_{\lambda_o}^{\alpha_{\lambda_o}} G_{\lambda_o}] = E[s_{\lambda}^{\alpha_{\lambda,\mathrm{eff}}} G_{\lambda}]. \tag{A.3}$$

Expansion of the above equation gives

$$E[s_{\lambda_o}^{\alpha_{\lambda_o}}]E[G_{\lambda_o}] + \mathrm{COV}[s_{\lambda_o}^{\alpha_{\lambda_o}}, G_{\lambda_o}] = E[s_{\lambda}^{\alpha_{\lambda,\mathrm{eff}}}]E[G_{\lambda}] + \mathrm{COV}[s_{\lambda}^{\alpha_{\lambda,\mathrm{eff}}}, G_{\lambda}]. \tag{A.4}$$

Since soil moisture is strongly correlated with coincident precipitation or net input of water to the ground, it is not unreasonable to assume that the covariance of $s_{\lambda_o}^{\alpha_{\lambda_o}}$ and G_{λ_o} is approximately equal to the covariance of $s_{\lambda}^{\alpha_{\lambda,\mathrm{eff}}}$ and G_{λ}. Further, noting that the expected value of G at scale λ_o over some domain is equal to the expected value of G at scale λ over that same domain (i.e., $E[G_{\lambda_o}] = E[G_{\lambda}]$), we arrive at

$$E[s_{\lambda_o}^{\alpha_{\lambda_o}}] \cong E[s_{\lambda}^{\alpha_{\lambda,\mathrm{eff}}}], \tag{A.5}$$

which is the same as Eq. (6) and therefore results in the same Eq. (9). This demonstrates that there is no loss of generality in assuming that the proportionality factor in Eq. (1) is a constant versus a more general spatially variable field. The assumption made above was that the covariance between relative soil moisture s and effective precipitation G is scale-independent. This is a reasonable assumption given the high degree of covariation of these variables at all scales.

References

[1] Bronstert A, Bardossy A. The role of spatial variability of soil moisture for modelling surface runoff generation at the small catchment scale. Hydro Earth Sys Sci 1999;3(4):505–16.

[2] Chen F, Avissar R. The impact of land-surface wetness heterogeneity on mesoscale heat fluxes. J Appl Meteoro 1994;33(11):1323–40.

[3] Chen F, Avissar R. Impact of land-surface moisture variability on local shallow convective cumulus and precipitation in large-scale models. J Appl Meteoro 1994;33(12):1382–401.

[4] Cosh MH, Brutsaert W. Aspects of soil moisture variability in the Washita '92 study region. J Geophys Res 1999;104(D16):19751–7.

[5] Dickinson RE, Henderson-Sellers A, Kennedy PJ. Biosphere–Atmosphere Transfer Scheme (BATS) Version 1e as coupled to the NCAR community climate model. NCAR Technical Note NCAR/TN-387+STR, 1993.

[6] Entekhabi D, Asrar GR, Betts AK, Beven KJ, Bras RL, Duffy CJ, et al. An agenda for land surface hydrology research and a call for the second international hydrological decade. Bull Am Meteoro Soc 1999;80(10):2043–58.

[7] Famiglietti JS, Wood EF. Effects of spatial variability and scale on areally averaged evapotranspiration. Water Resour Res 1995;31(3):699–712.

[8] Famiglietti JS, Devereaux JA, Laymon CA, Tsegaye T, Houser PR, Jackson TJ, et al. Ground-based investigation of soil moisture variability within remote sensing footprints during the Southern Great Plains 1997 (SGP97) Hydrology Experiment. Water Resour Res 1999;35(6):1839–51.

[9] Friedl MA. Examining the effects of sensor resolution and subpixel heterogeneity on spectral vegetation indices: implications for biophysical modeling. In: Quattrochi DA, Goodchild MF, editors. Scale in remote sensing and GIS. New York: CRC Lewis; 1997.

[10] Ghan SJ, Liljegren JC, Shaw WJ, Hubbe JH, Doran JC. Influence of subgrid variability on surface hydrology. J Climate 1997;10(12):3157–66.

[11] Hu Z, Islam S, Cheng Y. Statistical characterization of remotely sensed soil moisture images. Remote Sensing Environ 1997;61:310–8.

[12] Jackson TJ, Le Vine DM, Swift CT, Schmugge TJ, Schiebe FR. Large area mapping of soil moisture using the ESTAR passive microwave radiometer in Washita '92. Remote Sensing Environ 1995;53:27–37.

[13] Jackson TJ, Le Vine DM, Hsu AY, Oldak A, Starks PJ, Swift CT, et al. Soil moisture mapping at regional scales using microwave radiometry: the Southern Great Plains Hydrology Experiment. IEEE Trans Geosci Remote Sensing 1999;37:2136–51.

[14] Kustas WP, Jackson TJ. The impact on area-averaged heat fluxes from using remotely sensed data at different resolutions: a case study with Washita '92 data. Water Resour Res 1999;35(5):1539–50.

[15] Nykanen DK. Space–time variability of rainfall and soil moisture in coupled land–atmosphere modeling: issues of scale and effect on predicted water and energy fluxes. PhD thesis, University of Minnesota, Minneapolis, 2000.

[16] Nykanen DK, Foufoula-Georgiou E, Lapenta WM. Impact of small-scale rainfall variability on larger-scale spatial organization of land–atmosphere fluxes. J Hydrometeoro 2001;2(2):105–21.

[17] Rodriguez-Iturbe I, Vogel GK, Rigon R, Entekhabi D, Castelli F, Rinaldo A. On the spatial organization of soil moisture fields. Geophys Res Lett 1995;22(20):2757–60.

[18] Sivapalan M, Woods RA. Evaluation of the effects of general circulation models' subgrid variability and patchiness of rainfall and soil moisture on land surface water balance fluxes. In: Kalma

JD, Sivapalan M, editors. Advances in hydrological processes: scale issues in hydrological modelling. Chichester: Wiley; 1995.

[19] Su Z, Pelgrum H, Menenti M. Aggregation effects of surface heterogeneity in land surface processes. Hydro Earth Sys Sci 1999;3(4):549–63.

[20] Yang Z, Dickinson RE. Description of the Biosphere–Atmosphere Transfer Scheme (BATS) for the soil moisture workshop and evaluation of its performance. Global and Planetary Change 1996;13:117–34.